

## JAS1101 Final Report - Kinematics and Membership of the SMC Norther Over-Density (SMCNOD)

DINGDING WANG<sup>1</sup>

<sup>1</sup>*Department of Astronomy and Astrophysics, University of Toronto*

### ABSTRACT

In this report, we present the latest spectroscopic observations of the recently discovered stellar overdensity near the northern edge of the Small Magellanic Cloud (SMCNOD), taken as part of the Southern Stellar Stream Spectroscopic Survey (S5). A full kinematic analysis, including Gaia DR3 proper motions, was conducted. We model the candidate members of SMCNOD with a mixture model (stellar overdensity and MW background) in kinematics, metallicity, and proper motion space. The method does not require prior knowledge of stellar overdensity membership. This is the first study of accurate kinematics of SMCNOD, and our obtained metallicity is in agreement with the median metallicity of the nearby old SMC population. Further, we investigated the origin of SMCNOD with variable stars from the fourth release of the Optical Gravitational Lensing Experiment (OGLE), and analyzed the potential association of Eclipsing Binaries, Anomalous Cepheids, RR Lyrae stars, and Classical Cepheids with the stellar overdensity using their spatial distribution. Based on the spatial distribution of variable stars that are likely member stars of SMCNOD, we confirm the most likely origin of the stellar overdensity to be in the SMC itself, primarily composed of intermediate-age stars and somewhat older stars.

### 1. INTRODUCTION

The Magellanic Clouds (MCs) are the largest satellites of the Milky Way (MW), and the only irregular galaxies in its immediate surroundings. It has been shown to be quite rare for the existence of two satellites close to a Milky-Way-sized halo to be such gas-rich and massive (Liu et al. 2011). The MCs are embedded within a common envelope of neutral hydrogen, indicating interactions among the galaxies. It is also believed that the MCs have had interactions with the MW (Murai & Fujimoto 1986). Understanding the evolutionary history of the Magellanic Clouds requires an in-depth exploration and description of the stellar composition of its outer regions, which is ultimately key to tracing the age and nature of past interactions (Martínez-Delgado et al. 2019).

The SMC is a smaller counterpart of the LMC, and previous research suggests that the initial total mass of SMC is  $6.5 \times 10^9 M_{\odot}$  (Bekki & Stanimirović 2009). Compared with the LMC, the SMC has a more intricate structure with complex dynamics and kinematics. It is more metal-poor than the LMC(Carrera et al. 2008), and presents a peculiar history of star formation with conspicuous enhancements at various epochs (Noël et al. 2009).

In 2017, a small stellar overdensity 8 degrees north of the center of the SMC, was found by (Pieres et al.

2017). With the data from the Dark Energy Survey (2016) and the follow-up imaging performed with the Dark Energy Camera (Flaugher et al. 2015) as part of MAGellanic SatellITEsSurvey - MagLiteS (Drlica-Wagner et al. 2016), they traced and investigated this stellar overdensity. Pieres et al. (2017) named this newly-discovered feature of SMC the Small Magellanic Cloud Northern Over-Density(SMCNOD). According to Pieres et al. (2017), the SMCNOD is indistinguishable in age, metallicity, and distance from the nearby SMC stars. It contains primarily the intermediate-age stars ( $\sim 6$  Gyr with metallicity of  $Z=0.001$ ), with a small fraction of young stars ( $\sim 1$  Gyr,  $Z=0.01$ ). The estimated equatorial center coordinate of SMCNOD is  $R.A_{J2000} = 12.00$  deg and  $Dec_{J2000} = -64.80$  deg. Based on its colour-magnitude diagram(CMD), Pieres et al. (2017) showed that the SMCNOD distance modulus is indistinguishable from that of the SMC, (i.e.  $(m - M)_0^{\text{SMC}} = 18.96 \pm 0.02$  following the recommendation by (Grij & Bono 2015)).

The central questions of the follow-up studies of SMCNOD include the evaluation of its accurate kinematics, metallicity and membership. With these properties, we could answer the question of whether the origin of this stellar overdensity can be explained by the material pulled from the SMCdisc through tidal stripping, proposed by Pieres et al. (2017) to be the most likely scenario.

In this paper, we present new spectroscopic observations of SMCNOD from the Southern Stellar Stream Spectroscopic Survey(S<sup>5</sup>; [Li et al. \(2019\)](#)). Utilizing the 2-degree wide field of view and 350 science fibers of the 2dF fiber positioner, we have obtained accurate kinematics and metallicity properties of SMCNOD. As part of our analysis, we have also included the substantially improved proper motions from Gaia DR3 ([Gaia Collaboration et al. 2016, 2022](#)), and variable stars OGLE-IV photometric data ([Soszy'nski et al. 2017](#)).

The data sources and selection criteria are discussed in Section 2. In Section 3, we describe the statistical analysis of the stellar population and define the model and tools for the membership probability computation. We show the results from posterior distribution in Section 4, and discuss the origin of SMCNOD in Section 5. In Section 6, we summarise our findings.

## 2. DATA

The SMCNOD member stars are selected using the radial velocities (RVs) from the Southern Stellar Stream Spectroscopic Survey ( $S^5$  [Li et al. \(2019\)](#)) and proper motions (PMs) from *Gaia* DR3 ([Gaia Collaboration et al. 2016, 2022](#)). We also checked the quality of stellar membership with DECam photometry magnitudes from DECaLS DR9 ([Dey et al. 2019](#)) with an isochrone ( $\sim 6$  Gyr with metallicity of  $Z=0.001$ ) on the color-magnitude diagram (CMD).

To further study the origin of this stellar overdensity with the properties obtained from analysis of  $S^5$  data, we exploited variable stars from the fourth release of the Optical Gravitational Lensing Experiment (OGLE). Following the workflow of [Prudil et al. \(2018\)](#), we investigated the potential association of these variable stars with the SMCNOD using their spatial distribution.

As a limitation of using data from different surveys, we were not able to cross match the SMCNOD member stars from  $S^5$  with selected variable stars from OGLE. However, the study still provides insights on membership probability of these variable stars, as well as the origin of SMCNOD.

### 2.1. Southern Stellar Stream Spectroscopic Survey $S^5$

$S^5$  is a spectroscopic survey of stars in the stellar streams of the southern sky, aiming to map their kinematics and chemistry.  $S^5$  has been observing likely stellar members of the streams with 2dF/AAOmega spectrograph on the 3.9-meter Anglo-Australian Telescope (AAT) at Siding Spring Observatory since 2018. Details on the  $S^5$  survey strategies and observation can be found in [Li et al. \(2019\)](#).

#### 2.1.1. Data Reduction and Analysis

With the latest data release of  $S^5$ , we imposed a combination of cuts on the raw data to ensure the sample stars are of high quality. We first selected stars within a radius cut of  $1.05^\circ$  region with respect to the SMCNOD center from [Pieres et al. \(2017\)](#). If multiple exposures were taken for a single star, we use the signal-to-noise ratio of the best individual exposure for the quality cut. The high quality stars satisfy either `best_sn_1700d > 4` or `best_sn_580v > 4` for their signal-to-noise ratio. As larger velocity errors are often substantially affected by the sky subtraction residuals, we also require the `vel_calib_std < 10 km/s`. We also require the selected sample to have a `good_star_pb > 0.5`, which indicates probability of a star to be good based on random forest trained on a set of parameters. Detailed definitions of parameters can be found in [Li et al. \(2019\)](#).

Through exploratory data analysis, we checked the on-sky distribution of the high-quality star sample as well as visualizations of interested variables. We first selected peak of radial velocity and proper motions based on the histogram and scatter plot of the data. Through objective rough member-selection, we remove most likely non-members from the sample data and prepare for investigation of SMCNOD member analysis. We obtained a radial velocity peak near  $V_{\text{helio}} = 90 \text{ km s}^{-1}$ , so we selected objective member stars within  $60 < V_{\text{helio}} < 125.5 \text{ km s}^{-1}$ . We also made a box cut of  $0 < \mu_\alpha \cos(\delta) < 1.5 \text{ mas yr}^{-1}$  and  $-1.75 < \mu_\delta < -0.6 \text{ mas yr}^{-1}$  for the proper motions.

Finally, we obtained a quality cut sample data with 370 stars, and an objective member selection sample data with 150 stars. Figure 1 displays the high-quality stars with selected member stars highlighted in blue, in spatial distribution, RV vs. [Fe/H], proper motion space and colour-magnitude diagram(CMD). We can see that the selected sample stars are not exactly overlapping with the isochrone of age = 6 Gyr and  $Z = 0.001$ , proposed by [Pieres et al. \(2017\)](#).

### 2.2. OGLE-IV photometric data

For the purpose of studying the origin of SMCNOD, we have explored the data of variable stars from the latest data release of the Optical Gravitational Lensing Experiment (OGLE) of the Magellanic Clouds. The OGLE project ([Soszy'nski et al. 2017](#)) is a long term project with the main goal of searching for the dark matter with microlensing phenomena. The Magellanic Clouds and the Galactic Bulge are natural locations for such search due to their rich background stars that are potential targets for microlensing. The OGLE photometric observations are conducted in the I and V passbands of the Johnson-Cousins photometric system.

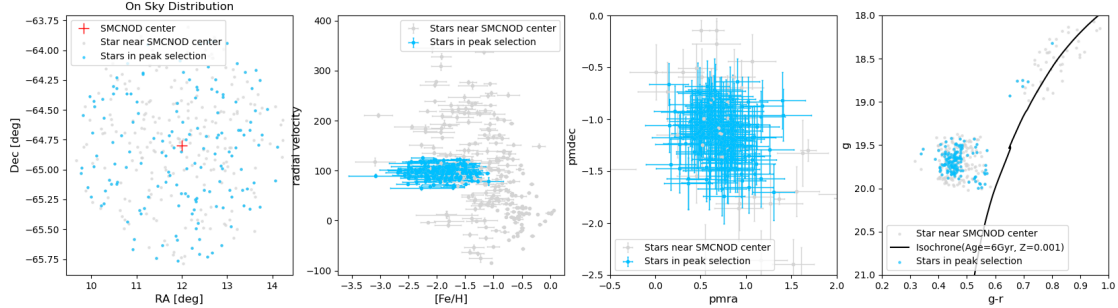


**Figure 1.** Objective member selection of SMCNOD with background of quality cut stars from  $S^5$ . First panel: the on-sky distribution of (RA, Dec) coordinates of selected stars. Second panel: RV vs. [Fe/H] distribution with error bars of selected stars. Third panel: Proper motions in RA and Dec space with error bars of selected stars. Last panel: colour-magnitude diagram(CMD) displaying an isochrone of age = 6 Gyr and Z = 0.001 with selected stars. In all panels, the objective selected members are colored in blue and the other stars in quality cut selection are in grey.

In the following subsections, we discuss the four types of variable stars from OGLE-IV for the SMC to study their association with the SMCNOD.

### 2.2.1. Eclipsing binaries

Eclipsing binaries(EBs) are useful tools to reveal unexpected structural details and time-related changes in the component stars. Recent observations have proven the potential of EBs to derive precise distances between the MW and nearby stellar systems for stellar population studies (Graczyk et al. 2014).

The OGLE-IV data release for eclipsing binaries (EBs) contains  $\sim 48000$  objects in the Magellanic system (Soszy’nski et al. 2017), of which 8401 belong to the SMC. The top panel of Figure 2 shows their spatial distribution in equatorial coordinates. We highlight the 6 EBs whose positions overlap with the SMCNOD region. Note that all these EBs belong to the eclipsing detached or semi-detached subtype.

### 2.2.2. Classical Cepheids

Classical Cepheids (CCs) are radially pulsating Population I variables, with high metallicities, and pulsation periods generally less than 10 days. They are comparatively young stars with masses of several times the solar mass. All Cepheids are luminous, yellow, horizontal branch stars that lie in the instability strip of the Hertzsprung-Russell diagram. Instabilities would result in their size and temperature changing giving rise to periodic variations in their luminosity.

The OGLE-IV data release for CCs contains  $\sim 9649$  objects in the Magellanic system, of which  $\sim 5000$  belong to the SMC. Figure 3 shows the celestial distribution of CCs in the SMC. We can see that none of the CCs overlaps with the SMCNOD region. They mainly concentrate in the central regions of the SMC, with only

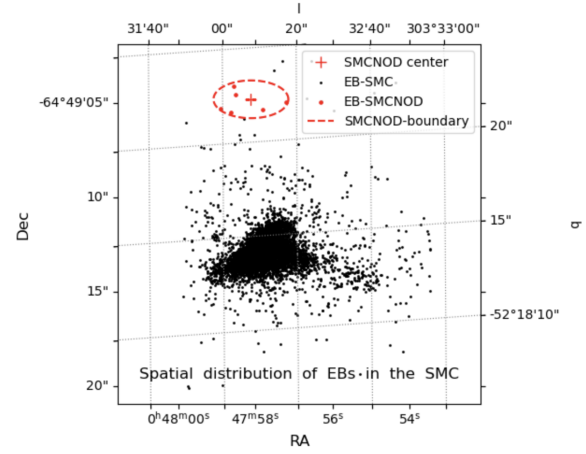


**Figure 2.** Spatial distribution for eclipsing binaries(EBs) in equatorial coordinates for the SMC represented by black dots. Red circles represent EBs that lie at similar coordinates as the SMCNOD. The red dash-dotted ellipse indicates the approximate position of stars around the SMCNOD center by Pieres et al. (2017).

a few located in the outskirts. The lack of CCs in the SMCNOD indicates a lack of comparatively young stars.

### 2.2.3. Anomalous Cepheids

Anomalous Cepheids (ACs) are relatively massive, up to 2 solar masses (Caputo et al. 2004), metal-deficient pulsating stars. They spread between classical and type II Cepheids in the period-luminosity diagram. Two leading hypotheses for the origin of anomalous Cepheids suggest that they are either intermediate-age stars with exceptionally low metallicity, or that they are coalesced old binary stars.

The OGLE-IV photometry for the SMC contains 119 ACs, and 4 ACs are located at the same range of coordinates as the SMCNOD. Figure 4 shows their spatial distribution. We can see that it is quite unusual for all

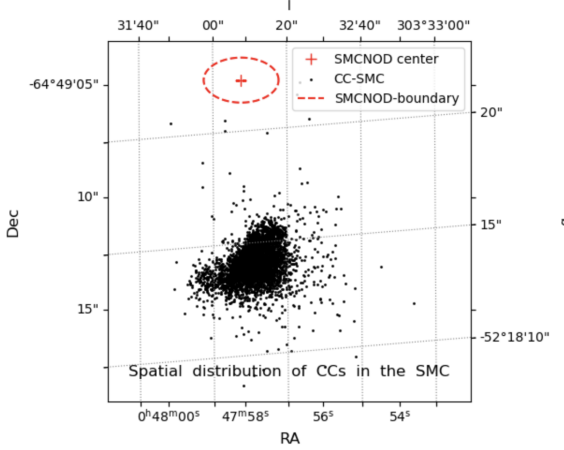


**Figure 3.** Spatial distribution for Classical Cepheids(CC)s in the SMC, similar to Figure 2. None of the CCs lie at similar coordinates as the SMCNOD. The red dash-dotted ellipse indicates the approximate position of stars around the SMCNOD center.

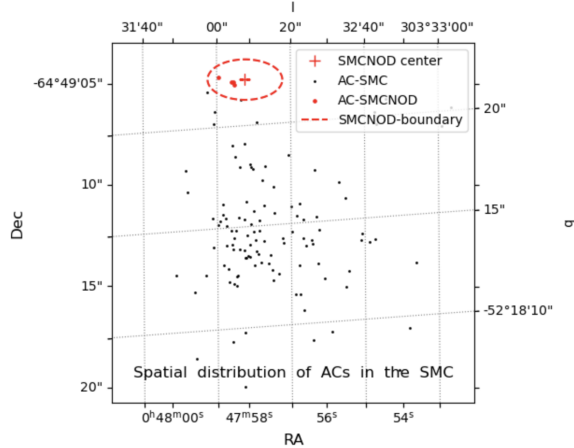


**Figure 4.** Spatial distribution of Anomalous Cepheids(ACs) in the SMC, similar to Figure 2

4 ACs to be the only few stars located in the outskirts of SMC.

#### 2.2.4. RR Lyrae stars

RR Lyrae stars are low metallicity (population II) stars that begin their lives with a mass and size similar to that of our Sun. They have typical ages of around 10 billion years, as they become RR Lyrae stars during the red giant phase, which is late in the evolution of the star. They are unambiguous indicators of populations older than 9 Gyr.

OGLE-IV contains over 45000 RR Lyrae stars in the Magellanic system, of which 6572 lie in the SMC. In our study, we only use the fundamental-mode RR Lyraes. Their spatial distribution is plotted in Figure 5. A to-

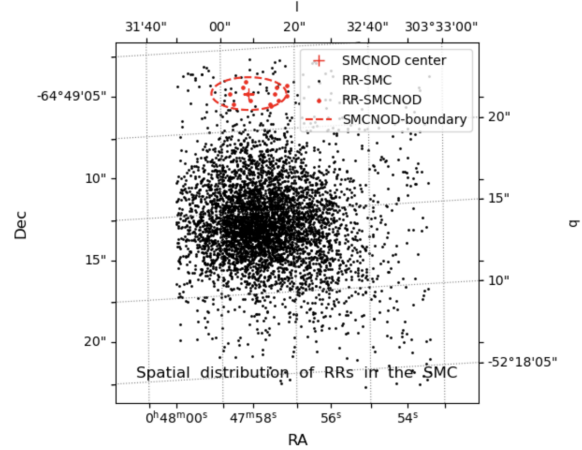


**Figure 5.** Spatial distribution of RR Lyrae stars in the SMC, similar to Figure 2

tal of 13 RR Lyrae stars overlap with the region of the SMCNOD.

### 3. METHODS

#### 3.1. Gaussian Mixture Model

A Gaussian mixture model is a simplified probabilistic model, which the assumption that data are all generated from a mixture of a finite number of Gaussian distributions with unknown parameters. In this study, stellar membership and kinematic properties are measured using a combination of radial velocity and metallicity, and Gaia DR3 proper motions.

We first generalized a pairwise plot with kernel density estimation (KDE) on scatter plots and histograms to incorporate information about the number of components and covariance of the variables. According to Figure 6, we can see that each variable has 2-3 components. In this study, we would fit the data with a 3-component mixture model: one SMCNOD component and two background components.

We also need to validate the distribution of the variables follow gaussian distribution. Q-Q plot, also called quantile-quantile plot, is a graphical tool to assess if a set of data plausibly came from some theoretical distribution. In this case, I run a statistical analysis that assumes our residuals are normally distributed, we can use a Normal Q-Q plot to check that assumption. It is a visual check and is somewhat subjective. But it allows us to see at-a-glance if our assumption is plausible, and if not, how the assumption is violated and what data points contribute to the violation. Based on Figure 7, we can see that the data points of all four variables fall on the 45-degree reference line, so we can safely move to use gaussian mixture models for our study.

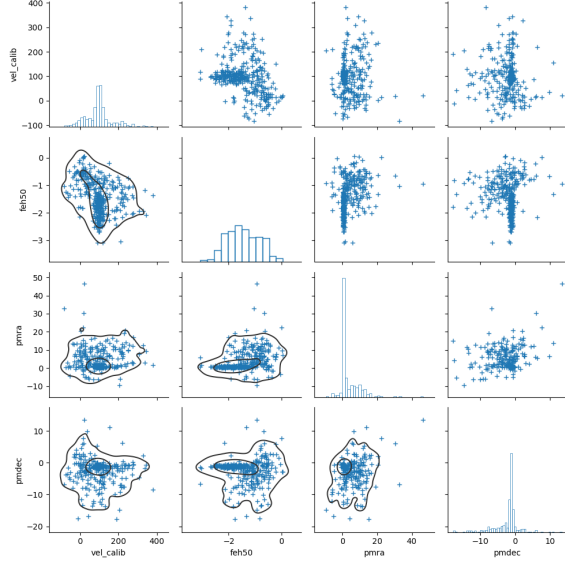


**Figure 6.** Plot pairwise relationships of radial velocity, metallicity and proper motion variables of quality cut stars from  $S^5$ . The pairs plot builds on two basic figures, the histogram and the scatter plot. On the diagonal, histograms allows us to see the distribution of a single variable. On the upper and lower triangles, the scatter plots show the relationship between two variables. The Kernel Distribution Estimation shows that the variables have 2-3 components.

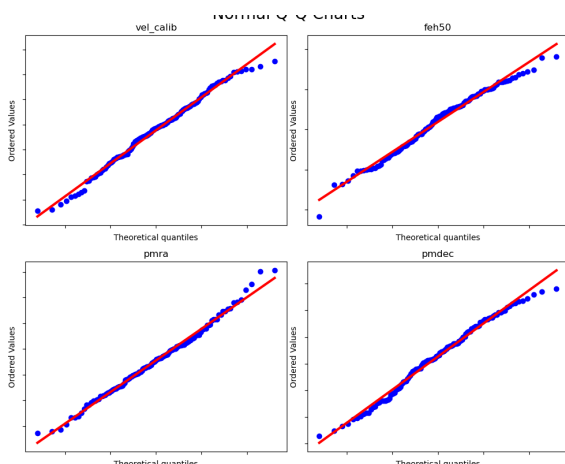


**Figure 7.** Normal Q-Q plot of radial velocity, metallicity and proper motion variables. With this quantile-quantile plot, we visually check that all the residuals of variables are normally distributed, so it is safe to move run a gaussian mixture model.

### 3.2. Bayesian Sampling

We model the candidate stars as a mixture model containing a satellite and two MW backgrounds, following the model described in Pace & Li (2019). The total

likelihood  $\mathcal{L}$  is:

$$\mathcal{L} = f_{\text{SMCNOD}} \mathcal{L}_{\text{SMCNOD}} + f_{\text{bg1}} \mathcal{L}_{\text{bg1}} + (1 - f_{\text{bg1}}) \mathcal{L}_{\text{bg2}}$$

where  $\mathcal{L}_{\text{SMCNOD}}$ ,  $\mathcal{L}_{\text{bg1}}$  and  $\mathcal{L}_{\text{bg2}}$  correspond to the SMCNOD stars and two MW background components respectively.  $f_{\text{SMCNOD}}$  is the fraction of stars in the SMCNOD component,  $f_{\text{bg1}}$  is the fraction of stars in the first MW background component.

Each likelihood term is decomposed into spatial proper motion parts:

$$\mathcal{L}_{\text{SMCNOD/MW}} = \mathcal{L}_{\text{spatial}} \mathcal{L}_{\text{PM}}$$

where  $\mathcal{L}_{\text{spatial}}$  and  $\mathcal{L}_{\text{PM}}$  are terms for the spatial and proper motion distributions respectively. The proper motion term is modeled as a multi-variate Gaussian:

$$\ln \mathcal{L}_{\text{PM}} = -\frac{1}{2}(\chi - \bar{\chi})^\top C^{-1}(\chi - \bar{\chi}) - \frac{1}{2} \ln (4\pi^2 \det C)$$

where  $\chi = (\mu_\alpha \cos \delta, \mu_\delta)$   $\bar{\chi} = (\overline{\mu_\alpha \cos \delta}, \overline{\mu_\delta})$  are respectively the data vector and the vector containing the systemic proper motion of the SMCNOD or MW background. The covariance matrix,  $C$ , includes the correlation between the proper motion errors and a term for the intrinsic proper motion dispersion:

$$C = \begin{bmatrix} \epsilon_{\mu_\alpha \cos \delta}^2 + \sigma_{\mu_\alpha \cos \delta}^2 & \epsilon_{\mu_\alpha \cos \delta \times \mu_\delta}^2 \\ \epsilon_{\mu_\alpha \cos \delta \times \mu_\delta}^2 & \epsilon_{\mu_\delta}^2 + \sigma_{\mu_\delta}^2 \end{bmatrix}$$

where  $\epsilon$  represents the proper motion errors and  $\sigma$  represents the intrinsic dispersions. We do not include intrinsic dispersion terms for the SMCNOD component as it is expected to be significantly smaller than the proper motion uncertainties.

We defined our full likelihood function with the following 16 parameters for SMCNOD and background components.

- pgal = fraction of stars in the galaxy
- pb1 = fraction of stars in the 1st background component
- pmra = Heliocentric proper motion, RA of the galaxy in mas/yr
- pmdec = Heliocentric proper motion, Dec of the galaxy in mas/yr
- vhel = mean velocity of the galaxy in km/s
- lsigv = log10 the velocity dispersion of the galaxy in km/s
- feh = mean metallicity of the galaxy in dex

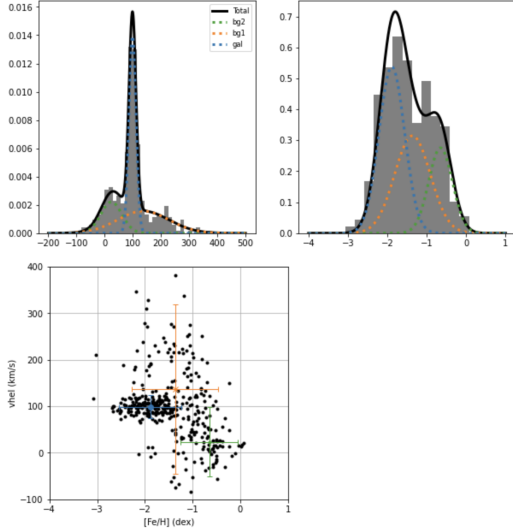


**Figure 8.** Projection of Optimize parameters on rv, [Fe/H]

- lsigfeh = log10 the metallicity dispersion of the galaxy in dex
- vbg1, lsigvbg1, fehbg1, lsigfeh1 = same parameters for 1st background component
- vbg2, lsigvbg2, fehbg2, lsigfeh2 = same parameters for 2nd background component

We used a Markov Chain Monte Carlo (MCMC) sampler method `emcee` (Foreman-Mackey et al. 2013) to sample the posterior distribution of parameters. Before moving to this step, we optimized our parameters with `scipy optimizers` (Virtanen et al. 2020) to improve efficiency of `emcee`. In Figure 8, we projected the parameters back into the observed space and they showed a good fit. This step is necessary because otherwise `emcee` would never give a right answer.

To determine a star's stellar overdensity membership, we take the ratio of SMCNOD likelihood to total likelihood:

$$p = \mathcal{L}_{\text{SMCNOD}} / ((1 - f_{\text{SMCNOD}}) \mathcal{L}_{\text{MW}} + f_{\text{SMCNOD}} \mathcal{L}_{\text{SMCNOD}})$$

This is computed for each star at each point in the posterior. We utilize the median value as the membership of the star.  $p$  represents the probability for the star to be a member of the SMCNOD population only considering its radial velocity, metallicity and proper motion. Stars are considered 'members' if they have  $p > 0.95$

## 4. RESULTS

Before moving to general results, we first examine the posterior result of mcmc sampling. With 64 walkers each taking 2000 steps and plus 100 steps for a burn-in period,

Figure 9 shows the posterior distribution of SMCNOD, and Figure 10 is a diagnostic plot showing the spatial distribution, RV v.s. [Fe/H], proper motions and CMD for member stars. From the quality cut sample of 370 stars, we obtained 175 high-probability member stars. The large number of members, the well-constrained posterior parameters (Figure 9 and the clear clustering of stars in proper motion space (Figure 10, third panel) all show that we have identified radial velocity, metallicity and the systemic proper motion of SMCNOD.

### 4.1. Systemic Velocity and Velocity Dispersion

In Figure 11, we present the posterior distribution of radial velocity and its dispersion of the SMCNOD. We compared the posterior result of radial velocity from both the quality-cut data and objective member selection data with Table 1. We use the 16th, 50th and 84th percentiles of the posterior distribution to derive the resulting values of parameters.

For the quality-cut stars, we find a systemic velocity of  $v_{\text{sys}} = 102.296^{+1.878}_{-1.878}$  km s $^{-1}$  and a velocity dispersion of  $\sigma_{v_{\text{sys}}} = 24.001^{+1.821}_{-1.821}$  km s $^{-1}$ . It is close to what we obtained from the objective member data, but the velocity dispersion is doubled. This is because we only considered hard cut-offs in peak selection for objective member data, so we did not consider some stars that may be members but are not strictly in the cut-off regions.

Variables	Quality cut	Member selection
vhel	$102.296 \pm 1.878$	$97.716 \pm 1.085$
sigv	$24.001 \pm 1.821$	$12.691 \pm 0.787$

**Table 1.** Posterior radial velocity and the velocity dispersion of both quality cut stars and objective member selection SMCNOD stars.

### 4.2. Metallicity

In Figure 12, we present the posterior distribution of metallicity and its dispersion of the SMCNOD. The posterior result of radial velocity from both the quality-cut data and objective member selection data are presented in Table 2. For the quality-cut stars, we find a metallicity of  $[Fe/H] = -1.900^{+0.029}_{-0.029}$  and a metallicity dispersion of  $\sigma_{[Fe/H]} = 0.325^{+0.033}_{-0.033}$ . The results are very close to the objective member selection.

### 4.3. Proper Motions

In Figure 13, we present the posterior distribution of proper motions of the SMCNOD. The posterior result of proper motions from both the quality-cut data and objective member selection data are presented in Table

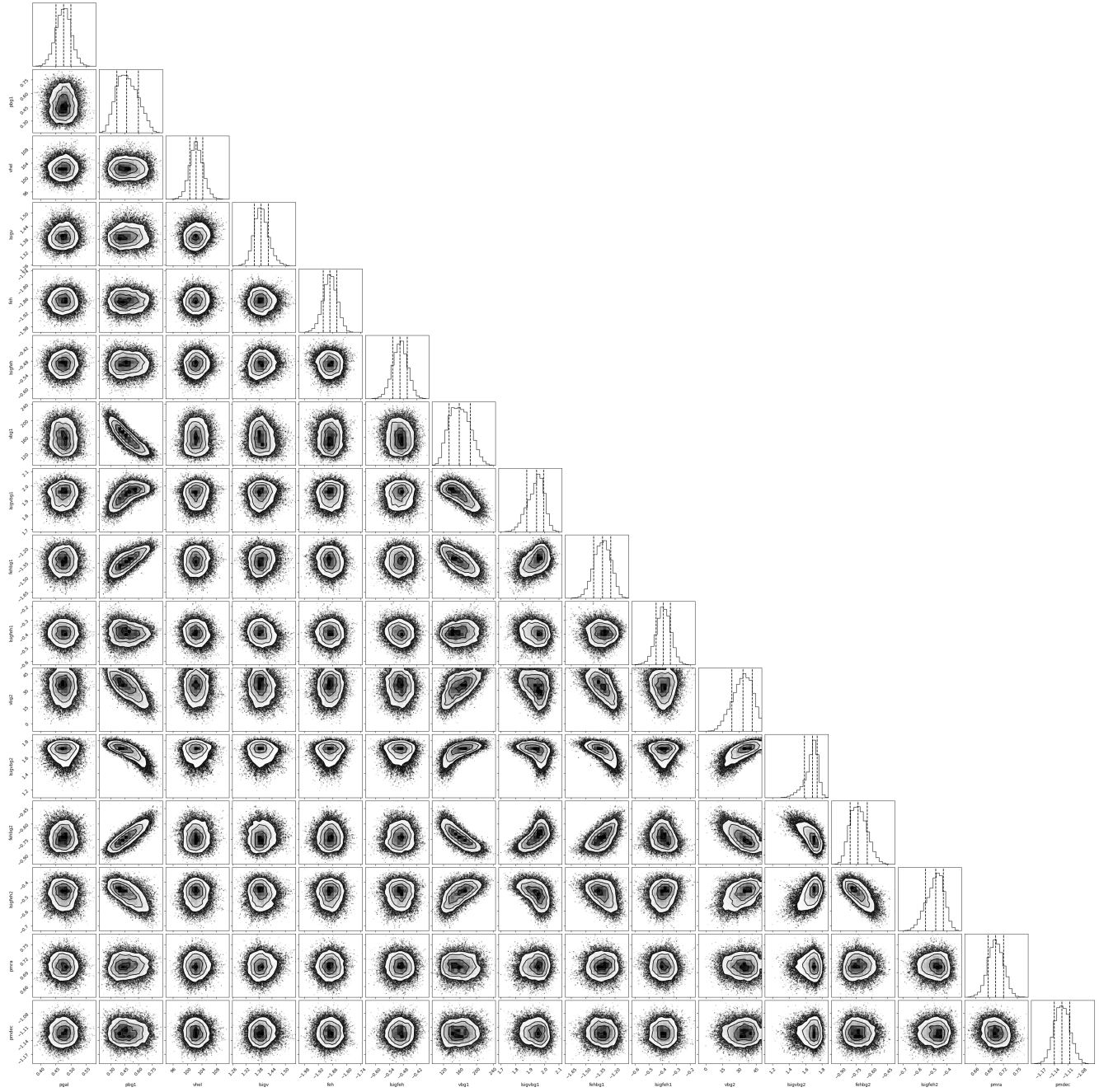


**Figure 9.** Posterior distribution of all 16 parameters. Details of the meaning of these parameters can be found in section 3.1. The contours enclose 39.4, 85.5, 98.9% of the posterior distribution corresponding to 1,2,3  $\sigma$  confidence intervals

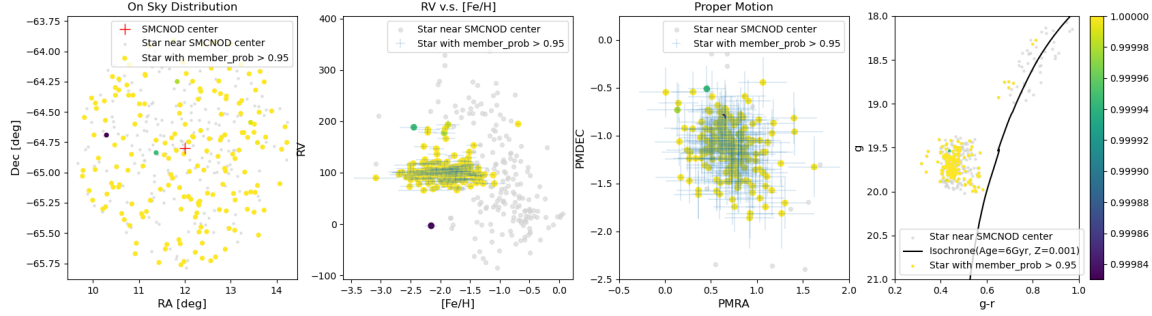


**Figure 10.** Diagnostic plots for SMCNOD. Panels from left to right show the spatial distribution, RV vs. [Fe/H] distribution, proper motion distribution, and color-color diagram for stars with membership probability  $\geq 0.95$ . We choose 0.95 to be the selection criteria of high-member probability stars instead of 0.5 because there is only one star with membership probability in the interval of [0.5, 0.95]. The grey dots are non-member stars within 1.05 half-light radius  $r_h$ . The solid black curve in the last panel shows an Dotter isochrone with age = 6 Gyr and Z = 0.001.

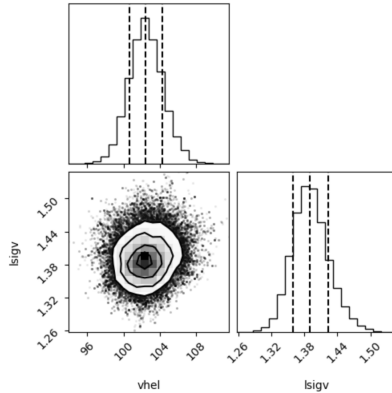


**Figure 11.** Posterior distribution of the radial velocity of the SMCNOD.

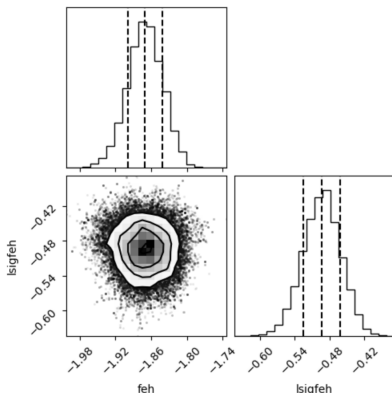


**Figure 12.** Posterior distribution of the metallicity of the SMCNOD.

3. For the quality-cut stars, we find a proper motions of  $[PMRA] = 0.703^{+0.016}_{-0.016}$  and  $[PMDEC] = -1.123^{+0.017}_{-0.017}$ . The results are also very close to the objective member selection.

#### 4.4. Spatial Distribution of Variable stars

Variables	Quality cut	Member selection
feh	$-1.900 \pm 0.029$	$-1.906 \pm 0.029$
sigfeh	$0.325 \pm 0.033$	$0.305 \pm 0.023$

**Table 2.** Posterior metallicity and metallicity dispersion of both quality cut stars and objective member selection SMCNOD stars.

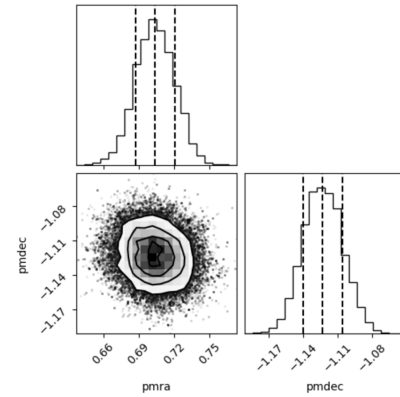


**Figure 13.** Posterior distribution of the proper motions of the SMCNOD.

Variables	Quality cut	Member selection
pmra	$0.703 \pm 0.016$	$0.702 \pm 0.016$
pmdec	$-1.123 \pm 0.017$	$-1.124 \pm 0.017$

**Table 3.** Posterior proper motions of both quality cut stars and objective member selection SMCNOD stars.

In order to test whether the variable stars could plausibly be a part of the SMCNOD, we visualize their on-sky spatial distribution with Figure 14. Due to the time limitation for this study, we did not numerically calculate their accurate distances to the SMCNOD center. From Figure 14, we can see that 4 RR-Lyrae stars, 3 Anoma-

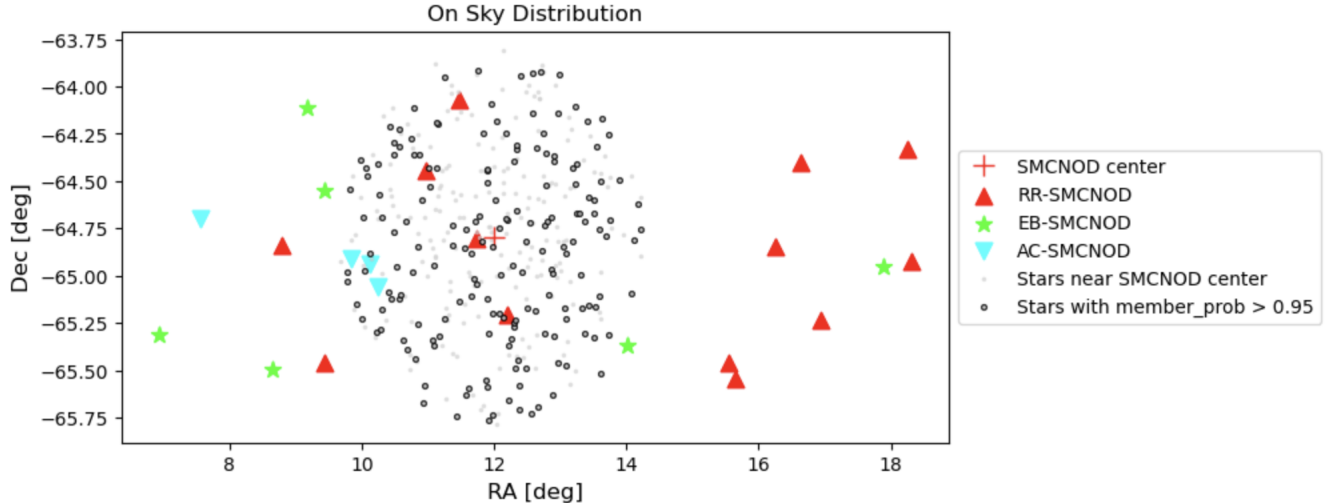


**Figure 14.** On-sky distribution of Variables Stars near SMCNOD centre from the OGLE-IV survey.

lous Cepheids, and 1 Eclipsing Binaries overlap with our selected member region.

To determine individual membership probability, we would need additional information about the radial velocity, metallicity, and proper motion data for each variable star. Unfortunately, neither of these is currently available with OGLE-IV. Although we aim to numerically calculate these properties following the procedure of Prudil et al. (2018), we propose tentative membership of these 8 variable stars with the SMCNOD for discussions.

## 5. DISCUSSION

### 5.1. Comparison to previous results

To December 2022, there have only been 2 papers published on SMCNOD, which makes it difficult to compare our kinematics results with previous literature. Although we find the metallicity of SMCNOD ( $[Fe/H]_{SMCNOD} = -1.90 \pm 0.03\text{dex}$ ) is 0.2 dex more metal-poor than the median metallicity of the SMC old population based on 1831 RR Lyrae stars derived by Haschke et al. (2012) ( $[Fe/H]_{SMC} = -1.70 \pm 0.27\text{dex}$ ), our result has a significantly lower uncertainty.

### 5.2. Origin of SMCNOD

We found 3 rather spatially concentrated Anomalous Cepheids, 4 evenly dispersed RR Lyrae stars, and one Eclipsing Binary to be most likely members of the SMCNOD. Different from the conclusion in Prudil et al. (2018), which found 4 Anomalous Cepheids and 8 RR Lyrae stars to be likely members of this stellar overdensity, we have fewer members for both Anomalous Cepheids and RR Lyrae stars, but a new discovery of Eclipsing Binary.

According to Figure 5, the RR Lyrae stars are evenly distributed across the outskirts of the SMC. The probability of finding four of them at the location of the SMCNOD is significantly higher than in the case of ACs, which occur rarely in the SMC outskirts based on Figure 4. Figure 15 also validates the overlap among selected member stars in the SMCNOD from  $S^5$ , RR Lyrae stars and Anomalous Cepheids from the OGLE survey.

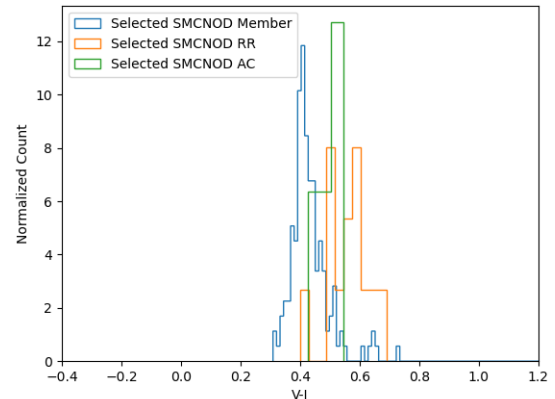


**Figure 15.** Color-magnitude diagram for SMCNOD

Although more analysis needs to be done for an accurate conclusion of the SMCNOD origin, we have shown in our study that the SMCNOD can be traced with old RR Lyrae stars and intermediate-age Anomalous Cepheids. The density of variable stars in the SMCNOD, SMC outskirts and the main body of SMC suggest that the origin of SMCNOD is most likely to be in the SMC itself, primarily composed of intermediate-age stars and somewhat older stars.

## 6. SUMMARY AND CONCLUSIONS

In this study, we present new AAT/2dF spectroscopy in the Small Magellanic Cloud Northern Over-Density(SMCNOD). We perform a detailed kinematic analysis including astrometry from *Gaia DR3*. With a sample of 370 high-quality stars, we obtained 175 stars with high membership probability. We found 3 rather spatially concentrated Anomalous Cepheids, 4 evenly dispersed RR Lyrae stars, and one Eclipsing Binary to be most likely members of the SMCNOD. The mem-

bership of these variable stars are tentative because more future analysis on their kinematics, metallicity and proper motions are required. We showed that the SMCNOD can be traced with the AC stars and RR Lyrae stars, suggesting the SMCNOD is primarily composed of intermediate-age stars and older stars. The density of variable stars in the SMCNOD, SMC outskirts, and the main body of SMC suggest that the origin of SMCNOD is most likely to be in the SMC itself.

## REFERENCES

- 2016, Monthly Notices of the Royal Astronomical Society, 460, 1270, doi: [10.1093/mnras/stw641](https://doi.org/10.1093/mnras/stw641)
- Bekki, K., & Stanimirović, S. 2009, MNRAS, 395, 342, doi: [10.1111/j.1365-2966.2009.14514.x](https://doi.org/10.1111/j.1365-2966.2009.14514.x)
- Caputo, F., Castellani, V., Degl'Innocenti, S., Fiorentino, G., & Marconi, M. 2004, Astronomy and Astrophysics, 424, 927–934, doi: [10.1051/0004-6361:20040307](https://doi.org/10.1051/0004-6361:20040307)
- Carrera, R., Gallart, C., Aparicio, A., et al. 2008, The Astronomical Journal, 136, 1039–1048, doi: [10.1088/0004-6256/136/3/1039](https://doi.org/10.1088/0004-6256/136/3/1039)
- Dey, A., Schlegel, D. J., Lang, D., et al. 2019, AJ, 157, 168, doi: [10.3847/1538-3881/ab089d](https://doi.org/10.3847/1538-3881/ab089d)
- Drlica-Wagner, A., Bechtol, K., Allam, S., et al. 2016, ApJL, 833, L5, doi: [10.3847/2041-8205/833/1/L5](https://doi.org/10.3847/2041-8205/833/1/L5)
- Flaugher, B., Diehl, H. T., Honscheid, K., et al. 2015, AJ, 150, 150, doi: [10.1088/0004-6256/150/5/150](https://doi.org/10.1088/0004-6256/150/5/150)
- Foreman-Mackey, D., Hogg, D. W., Lang, D., & Goodman, J. 2013, PASP, 125, 306, doi: [10.1086/670067](https://doi.org/10.1086/670067)
- Gaia Collaboration, Prusti, T., de Bruijne, J. H. J., et al. 2016, A&A, 595, A1, doi: [10.1051/0004-6361/201629272](https://doi.org/10.1051/0004-6361/201629272)
- Gaia Collaboration, Vallenari, A., Brown, A. G. A., et al. 2022, arXiv e-prints, arXiv:2208.00211. <https://arxiv.org/abs/2208.00211>
- Graczyk, D., Pietrzyński, G., Thompson, I. B., et al. 2014, ApJ, 780, 59, doi: [10.1088/0004-637X/780/1/59](https://doi.org/10.1088/0004-637X/780/1/59)
- Grijalva, R. d., & Bono, G. 2015, The Astronomical Journal, 149, 179, doi: [10.1088/0004-6256/149/6/179](https://doi.org/10.1088/0004-6256/149/6/179)
- Haschke, R., Grebel, E. K., Duffau, S., & Jin, S. 2012, The Astronomical Journal, 143, 48, doi: [10.1088/0004-6256/143/2/48](https://doi.org/10.1088/0004-6256/143/2/48)
- Li, T. S., Koposov, S. E., Zucker, D. B., et al. 2019, MNRAS, 490, 3508, doi: [10.1093/mnras/stz2731](https://doi.org/10.1093/mnras/stz2731)
- Liu, L., Gerke, B. F., Wechsler, R. H., Behroozi, P. S., & Busha, M. T. 2011, The Astrophysical Journal, 733, 62, doi: [10.1088/0004-637x/733/1/62](https://doi.org/10.1088/0004-637x/733/1/62)
- Martínez-Delgado, D., Vivas, A. K., Grebel, E. K., et al. 2019, Astronomy and Astrophysics, 631, A98, doi: [10.1051/0004-6361/201936021](https://doi.org/10.1051/0004-6361/201936021)
- Murai, T., & Fujimoto, M. 1986, Ap&SS, 119, 169, doi: [10.1007/BF00648839](https://doi.org/10.1007/BF00648839)
- Noël, N. E., Aparicio, A., Gallart, C., et al. 2009, The Astrophysical Journal, 705, 1260–1274, doi: [10.1088/0004-637x/705/2/1260](https://doi.org/10.1088/0004-637x/705/2/1260)
- Pace, A. B., & Li, T. S. 2019, ApJ, 875, 77, doi: [10.3847/1538-4357/ab0aee](https://doi.org/10.3847/1538-4357/ab0aee)
- Pieres, A., Santiago, B. X., Drlica-Wagner, A., et al. 2017, MNRAS, 468, 1349, doi: [10.1093/mnras/stx507](https://doi.org/10.1093/mnras/stx507)
- Prudil, Z., Grebel, E. K., Dé kány, I., & Smolec, R. 2018, Monthly Notices of the Royal Astronomical Society, 480, 669, doi: [10.1093/mnras/sty1885](https://doi.org/10.1093/mnras/sty1885)
- Soszyński, I., Udalski, A., Szymański, M. K., et al. 2017, arXiv: Solar and Stellar Astrophysics
- Virtanen, P., Gommers, R., Oliphant, T. E., et al. 2020, Nature Methods, 17, 261, doi: [10.1038/s41592-019-0686-2](https://doi.org/10.1038/s41592-019-0686-2)